# Ben Naim's four-arm model with density anomaly: Theory and computer simulations

Tomaz Urbic*

*University of Ljubljana, Faculty of Chemistry and Chemical Technology, Večna pot 113, SI-1000 Ljubljana, Slovenia*

(Received 11 April 2023; accepted 1 July 2023; published 31 July 2023)

Molecular dynamics, Wertheim's integral equation theory (IET), and thermodynamics perturbation theory (TPT) were used to study the thermodynamics and structure of particles interacting through angle-dependent potential. The particles are modeled as two-dimensional Lennard-Jones disks with four hydrogen bonding arms arranged symmetrically. The model was introduced by Ben-Naim and we call it the BN4 model. The BN4 model exhibits density anomaly and other anomalous properties similar to those in water and in the Mercedes-Benz (MB) model. The IET is based on the orientationally averaged version of the Ornstein-Zernike equation and correctly predicts the pair correlation function of the model at high temperatures. Both TPT and IET are in semiquantitative agreement with the simulation values of the molar volume, isothermal compressibility, thermal expansion coefficient, and heat capacity.

DOI: 10.1103/PhysRevE.108.014136

## I. INTRODUCTION

Water is special. It has some properties that distinguish it from other simpler liquids [1–4]. Liquid water covers three-fourths of the earth's surface. It controls the planet's geochemical cycles and is a dominant driver of biomolecules, drug interactions, and biological actions. It is the central compound in "green chemistry" and many industrial processes. Water exhibits many anomalous properties that affect life at a larger scale. Among the most important anomalies of pure water are a temperature of maximum density in the liquid phase, a lower density in the frozen state (ice) than in the liquid state, a minimum in the isothermal compressibility, and a large heat capacity. Water has almost universal solvent action [5,6]. Anomalous liquids are liquids that exhibit unexpected behavior upon variations of the thermodynamic conditions in comparison to normal (argon-like) liquids. Water is the classic example of those anomalous liquids. The anomalies in water appear to be related to the ability of water molecules to form tetrahedrally coordinated hydrogen bonds. There are two very distinct mechanisms that give rise to the anomalous properties, including angular-dependent interactions, such as oriented hydrogen bonding in water, which can result in density maximum because of the competition between tetrahedral order (low density) and translational order (high density). On the other hand, density anomaly was also observed for Ga [7], Bi [8], Te [9], S [10], Be, Mg, Ca, Sr, Ba, P, Se, Ce, Cs, Rb, Co, and Ge where the system lacks oriented bonding.

An understanding of hydrogen bonding is therefore crucial to understand the behavior and properties of water. Despite extensive theoretical and experimental works, how water's properties come from its molecular structure remains poorly understood. A large number of models of varying complexity have been developed and analyzed to model water's extraordinary properties [5,6,11–21]. The properties of water can be in principle determined with quantum-mechanical calculations [22,23]. This offers the highest degree of exactness, but it has a high computational cost. There have been two main approaches in explaining the properties of water. First is to perform computer simulations of atomically detailed models which aim for realistic detail and include variables describing van der Waals and Coulomb interactions, hydrogen bonding, etc. (reviewed in Ref. [13]). Many properties of water and aqueous solutions can also be explained by simpler models [24,25]. One class of such simpler models has been developed by Nezbeda and co-workers [12,26,27]. In our opinion, the simplest model for water is the so-called Mercedes–Benz (MB) model [28]. The MB model is a two-dimensional model which was originally proposed by Ben-Naim in 1971 [29,30]. In some publications it is also referred to as the BNMB (Ben-Naim-Mercedes-Benz) model. MB particles are modeled as Lennard-Jones (LJ) disks with three hydrogen bonding arms arranged as in the MB logo. The particles interact with other such waters through a LJ interaction and an orientation-dependent hydrogen bonding interaction through three radial arms. Ben-Naim in his paper also proposed a four-arm model [29,30] which is the topic of this study. We call this model the BN4 model. Interest in two-dimensional (2D) simplified models is due to insights that are not obtainable from all-atom computer simulations. Simpler models are more flexible in providing insights and illuminating concepts. The models also do not require large computer resources. Our interest in using the 2D models is that they serve as a test bed for developing analytical theories that might ultimately be useful for more realistic models. Another advantage of the 2D models, compared to more realistic water models, is that the underlying physical principles can be more readily explored and visualized in two dimensions. The MB model was also extensively studied with analytical methods like integral equation and thermodynamic perturbation theory [31–36] and statistical mechanic theory [37–39]. The phase diagram of the liquid part and percolation curve of the model was calculated and reported [40], and the MB model

*tomaz.urbic@fkkt.uni-lj.si

 

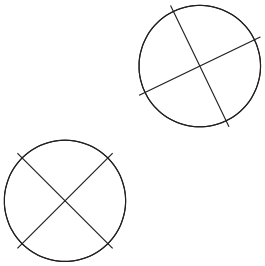

FIG. 1. The BN4 particles.

has also been used to study systems within small geometric spaces [36].

Computer simulations are an important tool to understand the properties of liquids, but they can be quite time consuming, even for simple 2D models. Because of this it is equally important to develop simplified analytical approaches. A theory has been developed for fluids where molecules associate into dimers and higher clusters due to the presence of highly directional attractive forces [41,42]. The theory has been successfully applied to a number of different three-dimensional fluid systems, including water and aqueous solutions (see, for example, Refs. [12,43,44] and references therein). Wertheim [41,42,45,46] proposed his statistical-mechanical approach for strongly associating systems of molecules as thermodynamics perturbation theory (TPT) and integral equation theory (IET). The Wertheim's TPT and orientationally averaged and angle-dependent IETs were applied for the MB model before. We found that both TPT and IET approaches gave good quantitative agreement with isothermal-isobaric (NPT) Monte Carlo results for the molar volume, isothermal compressibility, and other thermodynamic properties as a function of temperature.

In this paper, we explored properties of the BN4 model by computer simulations and Wertheim's theory. The outline of the paper is as follows. We present the model in Sec. II, and the details of the molecular dynamics simulations, overview of thermodynamics perturbation theory, and theory of integral equation are done in Sec. III. In Sec. IV we show and discuss the results, and we summarize everything in Sec. V.

## II. BN4 MODEL

The particles are modeled as two-dimensional disks with four bonding arms separated by an angle of 90° [29,30] which is fixed (see Fig. 1). The interaction between particles $i$ and $j$ is a sum of a LJ and a hydrogen bond (HB) or association contribution

$$U(\vec{X}_i, \vec{X}_j) = U_{\mathrm{LJ}}(r_{ij}) + U_{\mathrm{HB}}(\vec{X}_i, \vec{X}_j). \tag{1}$$

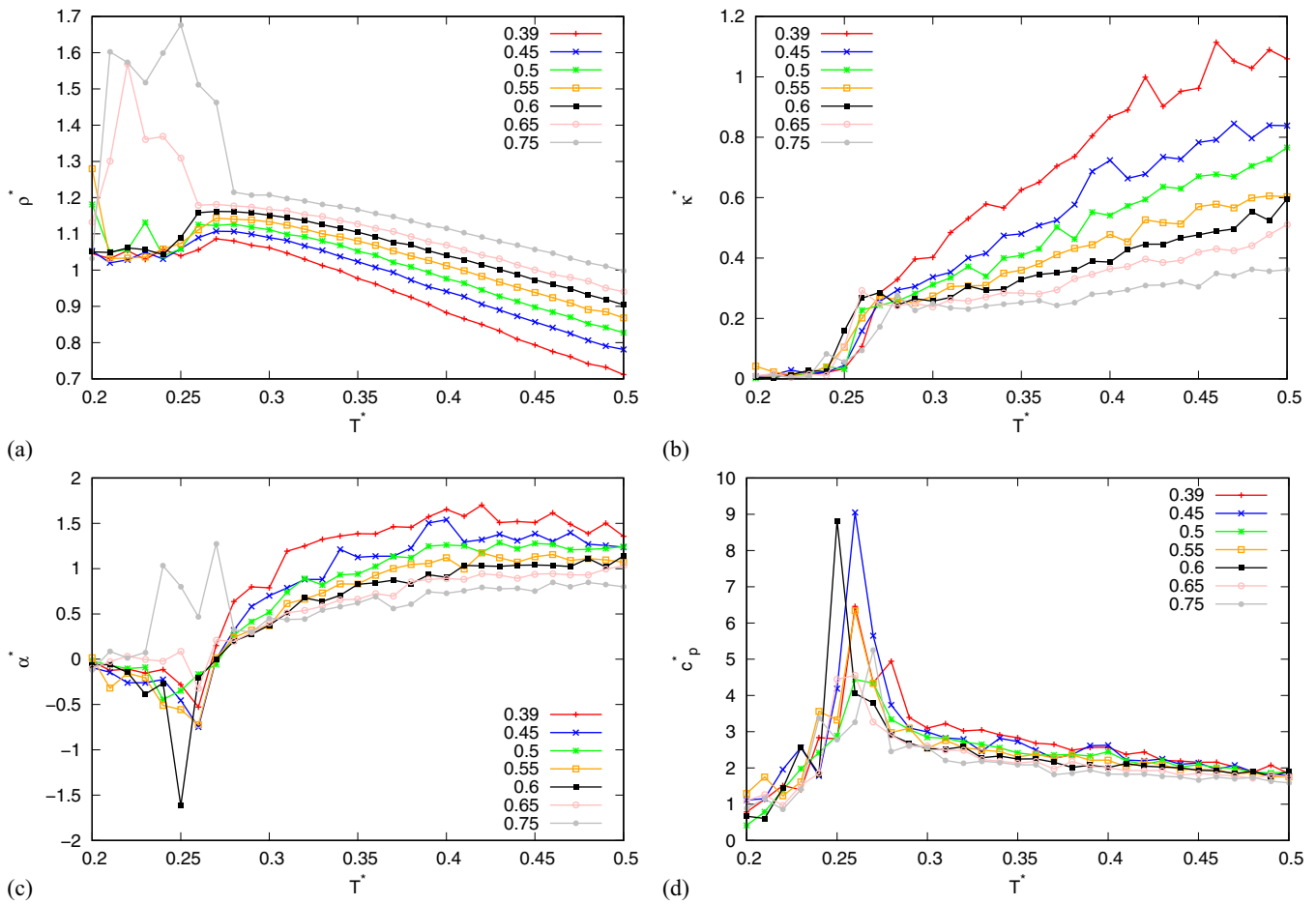


FIG. 2. Temperature dependence of (a) the density, (b) the isothermal compressibility multiplied by pressure, (c) the thermal expansion coefficient, and (d) the heat capacity for various pressures for $\sigma_{\mathrm{LJ}} = 0.7$.

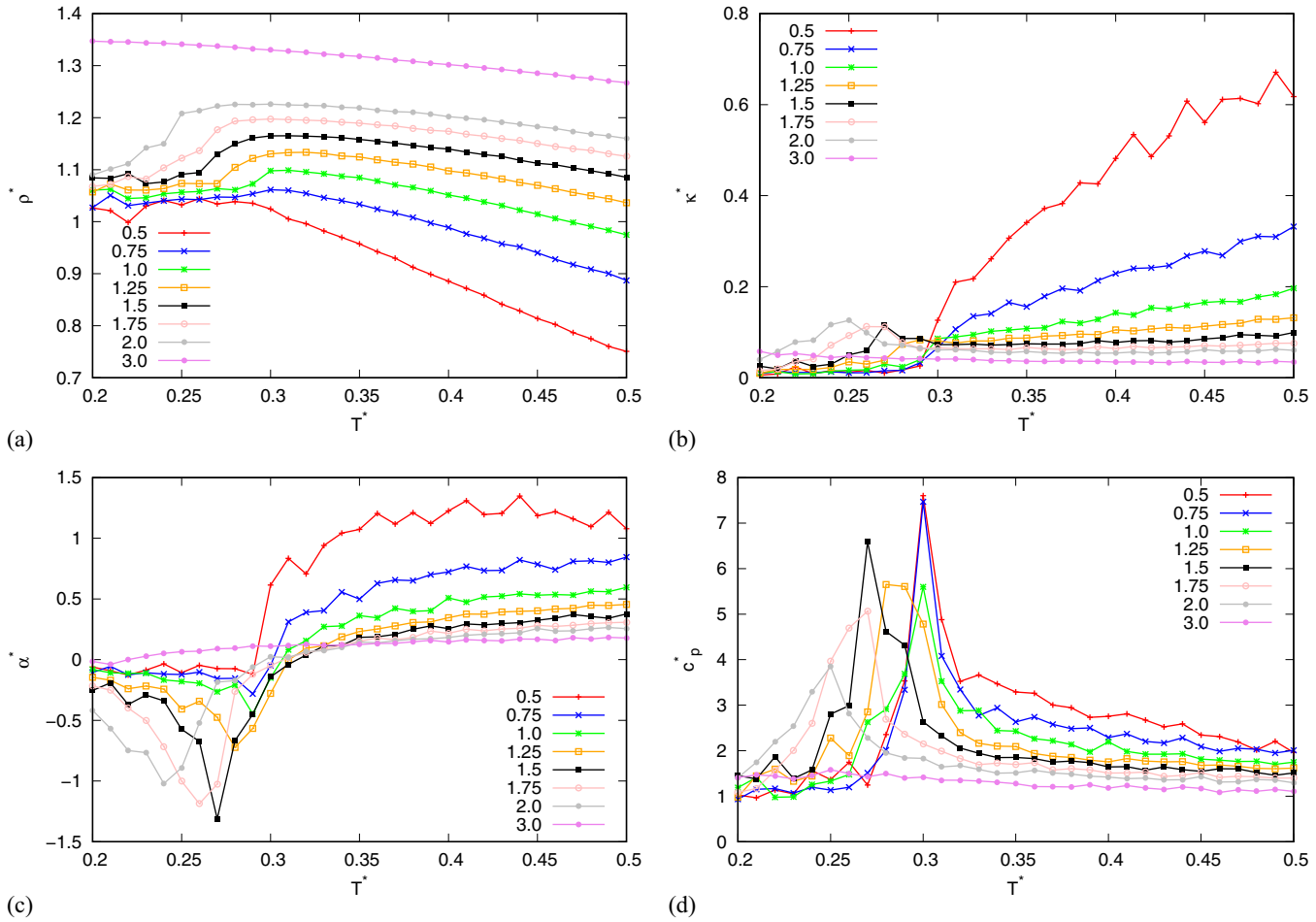


FIG. 3. Temperature dependence of (a) the density, (b) the isothermal compressibility multiplied by pressure, (c) the thermal expansion coefficient, and (d) the heat capacity for various pressures for $\sigma_{\mathrm{LJ}} = 0.8$.

$r_{ij}$ is the distance between particles $i$ and $j$. $\overrightarrow{X_i}$ and $\overrightarrow{X_j}$ are the vectors representing the coordinates and the orientation of the $i$th and $j$th particle. The LJ part has a standard form

$$U_{\mathrm{LJ}}(r_{ij}) = 4\varepsilon_{\mathrm{LJ}}\left(\left(\frac{\sigma_{\mathrm{LJ}}}{r_{ij}}\right)^{12} - \left(\frac{\sigma_{\mathrm{LJ}}}{r_{ij}}\right)^{6}\right). \tag{2}$$

$\sigma_{\mathrm{LJ}}$ and $\varepsilon_{\mathrm{LJ}}$ are the contact value of potential and the depth. The HB interaction is the sum of interactions $U_{\mathrm{HB}}^{kl}$ between all arms of different particles

$$U_{\mathrm{HB}}(\vec{X}_i, \vec{X}_j) = \sum_{k,l=1}^{4} U_{\mathrm{HB}}^{kl}(r_{ij}, \theta_i, \theta_j), \tag{3}$$

which is described by Gaussian function in distance and both angles

$$\begin{aligned} &U_{\mathrm{HB}}^{kl}(r_{ij}, \theta_i, \theta_j) \\ &\quad = \varepsilon_{\mathrm{HB}} G(r_{ij} - r_{\mathrm{HB}}) G(\vec{i}_k \vec{u}_{ij} - 1) G(\vec{j}_l \vec{u}_{ij} + 1) \qquad (4) \\ &\quad = \varepsilon_{\mathrm{HB}} G(r_{ij} - r_{\mathrm{HB}}) G\left\{ \cos\left[\theta_i + \frac{2\pi}{3}(k-1)\right] - 1 \right\} \\ &\qquad \times G\left\{ \cos\left[\theta_j + \frac{2\pi}{3}(l-1)\right] + 1 \right\}. \qquad (5) \end{aligned}$$

$\varepsilon_{\mathrm{HB}} = -1$ is a HB energy parameter and $r_{\mathrm{HB}} = 1$ is a characteristic length of HB. $\overrightarrow{u_{ij}}$ is the unit vector along $\overrightarrow{r_{ij}}$ and $\overrightarrow{i_k}$ is the unit vector representing the $k$th arm of the $i$th particle. $\theta_i$ is the orientation of $i$th particle with respect to $x$ axes. $G(x)$ is an unnormalized Gaussian function

$$G(x) = \exp\left(-\frac{x^2}{2\sigma^2}\right). \tag{6}$$

The strongest HB occurs when an arm of the first particle is co-linear with the arm of the second particle and the two arms point in opposing directions. The LJ well depth $\varepsilon_{\mathrm{LJ}}$ is 0.1 times the HB interaction energy $\varepsilon_{\mathrm{HB}}$ and the Lennard-Jones contact parameter $\sigma_{\mathrm{LJ}}$ is varied between $0.7r_{\mathrm{HB}}$ and $1.1r_{\mathrm{HB}}$. The width of Gaussian for distances and angles is $\sigma = 0.085r_{\mathrm{HB}}$.

## III. THEORY

### A. Molecular dynamics

Molecular dynamics simulations were used for the calculation of properties of the BN4 model. All calculations were done with our own software. The simulations were performed in canonical (NVT) isobaric-isothermal (NPT) ensembles with periodic boundary conditions and minimal image convention. Trajectory integration was done using the velocity Verlet integrator [47], and the length of the time step was

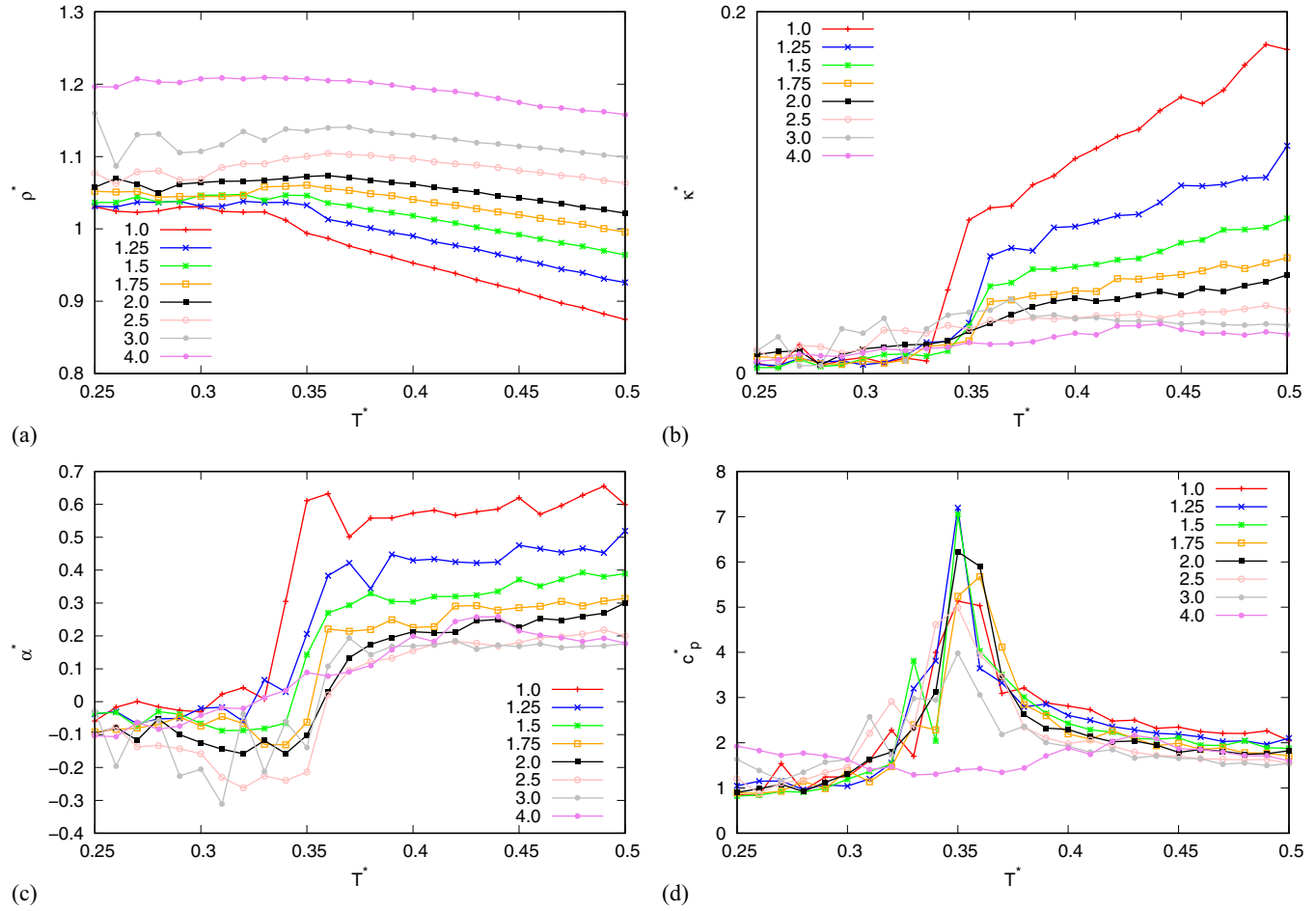


FIG. 4. Temperature dependence of (a) the density, (b) the isothermal compressibility multiplied by pressure, (c) the thermal expansion coefficient, and (d) the heat capacity for various pressures for $\sigma_{\mathrm{LJ}} = 0.9$.

set to 0.001 ($t^* = t\sqrt{\frac{\epsilon_{\mathrm{HB}}}{mr_{\mathrm{HB}}^2}}$). At the beginning the system was equilibrated by a simulation of a minimum of 50 000 steps in length, then the sampling phase of simulation was done in 20 series, where each series was a minimum of 50 000 steps long. During the sampling phase, structural and thermodynamic properties were calculated as an average over time. The number of particles in the system was between 100 and 400, which is equivalent to between 1000 and 8000 particles in three dimensions. The initial position of the particles was randomly selected in a way that particles did not overlap. Initial velocities were drawn from the Maxwell-Boltzmann distribution. In the equilibration phase, a simple velocity rescale was used to control the temperature. To keep the temperatures and pressures constant in production runs, we employed the Berendsen thermostat [48] with a time constant equal to 0.1 and the Berendsen barostat with same time constant as for thermostat. During the sampling phase thermodynamic quantities were calculated as statistical averages [49,50].

### B. Thermodynamic perturbation theory

Here we are briefly reviewing Wertheim's first-order perturbation theory [41,51], used previously [31–33] for the 2D MB model of water. We start with the Helmholtz free energy for BN4 particles, which is a sum of an ideal term $A_{id}$, a reference term $A_{\mathrm{LJ}}$, and a perturbation term $A_{\mathrm{HB}}$ which takes into account the association of BN4 molecules into hydrogen-bonded networks

$$\frac{A}{Nk_BT} = \frac{A_{id}}{Nk_BT} + \frac{A_{\mathrm{LJ}}}{Nk_BT} + \frac{A_{\mathrm{HB}}}{Nk_BT}. \tag{7}$$

$N$ is the number of BN4 particles, and $k_B$ and $T$ are Boltzmann's constant and temperature. The Lennard-Jones contribution $A_{\mathrm{LJ}}$ was calculated using the Barker-Henderson (BH) perturbation theory [31,49]. Within the BH theory, the reference system is the hard-disk system

$$\frac{A_{\mathrm{LJ}}}{Nk_BT} = \frac{A_{\mathrm{HD}}}{Nk_BT} + \frac{\rho}{2k_BT}\int_{\sigma_{\mathrm{LJ}}}^{\infty} g_{\mathrm{HD}}(r,\eta)u_{\mathrm{LJ}}(r)d\vec{r}\,. \tag{8}$$

$A_{\mathrm{HD}}$ is the hard-disk part of the Helmholtz free energy, $\rho$ is the number density of BN4 particles, $\eta$ is the packing fraction of the hard-disk reference system, and $g_{\mathrm{HD}}(r,\eta)$ is the pair distribution function of the hard-disk reference fluid [31]. The diameter of the hard-disk reference fluid was calculated by averaging the Boltzmann factor [31]. The contribution of hydrogen bonding to the Helmholtz free energy was calculated by

$$\frac{A_{\mathrm{HB}}}{Nk_BT} = 4\left(\log x - \frac{x}{2} + \frac{1}{2}\right). \tag{9}$$

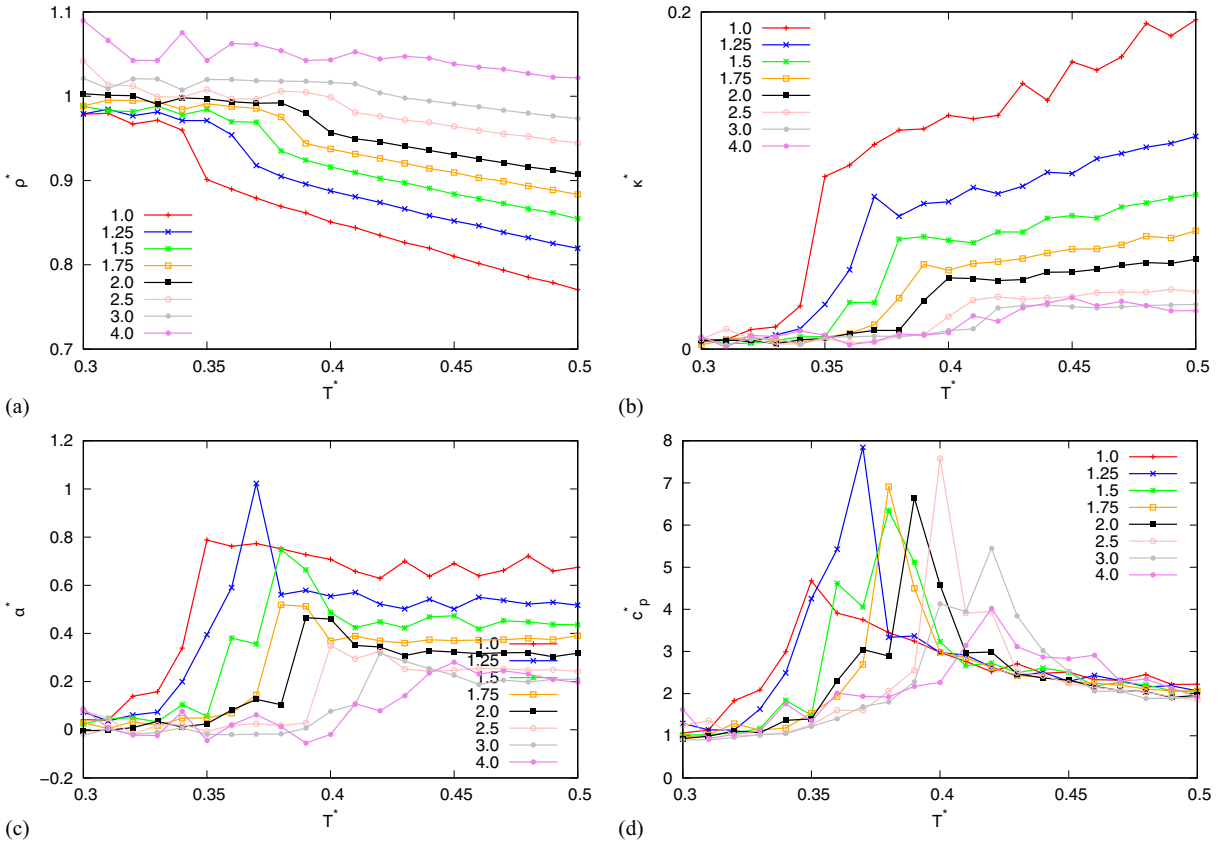


FIG. 5. Temperature dependence of (a) the density, (b) the isothermal compressibility multiplied by pressure, (c) the thermal expansion coefficient, and (d) the heat capacity for various pressures for $\sigma_{\mathrm{LJ}} = 1.0$.

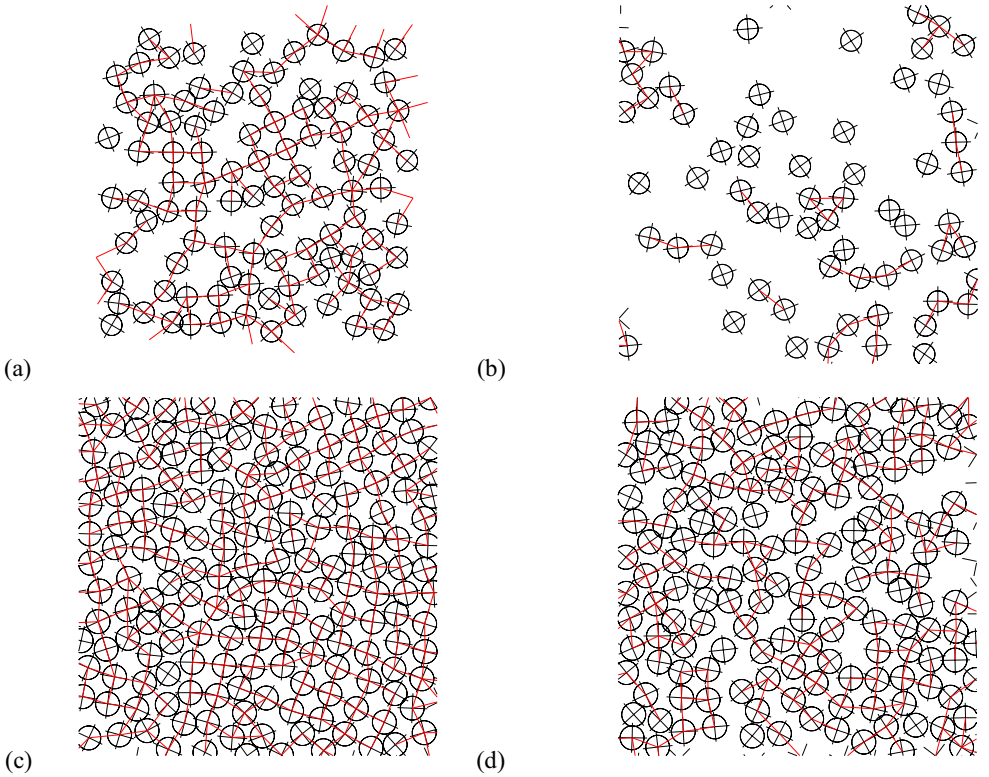


FIG. 6. Snapshots of the system for (a) $\sigma_{\mathrm{LJ}} = 0.7$, $p^* = 0.19$, $T^* = 0.30$; (b) $\sigma_{\mathrm{LJ}} = 0.7$, $p^* = 0.19$, $T^* = 0.45$; (c) $\sigma_{\mathrm{LJ}} = 0.8$, $p^* = 1.5$, $T^* = 0.30$; and (d) $\sigma_{\mathrm{LJ}} = 0.8$, $p^* = 1.5$, $T^* = 0.5$. Red lines connect BN4 molecules that form HBs.

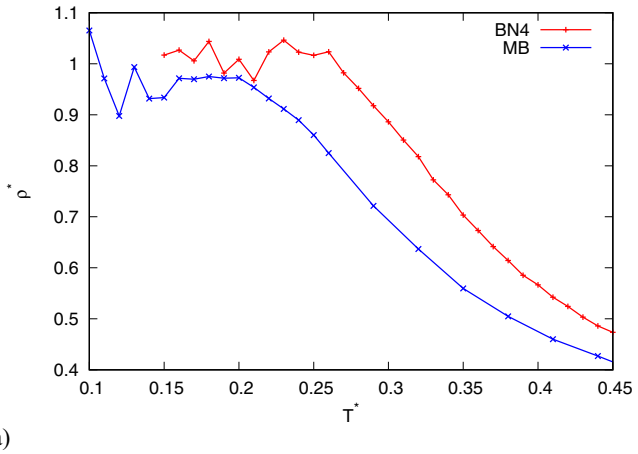


(a)

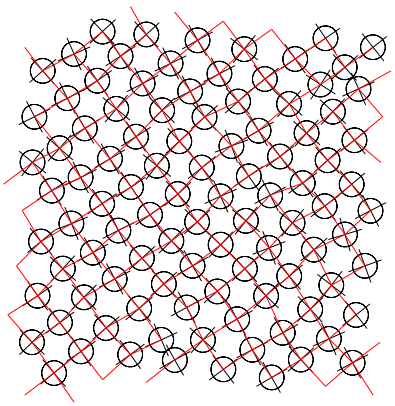

(b)

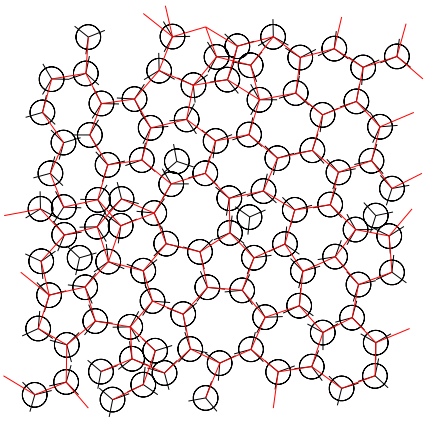

(c)

FIG. 7. (a) Comparison of density of MB and BN4 model for pressure $p^* = 0.19$. (b) Snapshots of the crystal phase of the BN4 system at $p^* = 0.19$ and $T^* = 0.25$ and (c) the crystal phase of the MB system at $p^* = 0.19$ and $T^* = 0.14$. Red lines connect molecules that form HBs.

$x$ is the fraction of molecules not bonded at one particular arm and is obtained from the mass-action law [41] in the form

$$x = \frac{1}{1 + 4\rho x \Delta}. \tag{10}$$

$\Delta$ is defined by [41,51]

$$\Delta = 2\pi \int g_{\mathrm{LJ}}(r, \rho) \bar{f}_{\mathrm{HB}}(r) r dr. \tag{11}$$

$\bar{f}_{\mathrm{HB}}(r)$ is an orientationally averaged Mayer function for the hydrogen bonding potential of one site. The pair distribution function $g_{\mathrm{LJ}}(r)$ is obtained by solving the Percus-Yevick equation for Lennard-Jones disks.

In the improved TPT [33], instead of the density $\rho$ we used the effective density $\rho^{ef}$ in Eqs. (7)–(11). The logic for this is that the particles cannot access the whole space in the system when they form bonds. When BN4 molecules form a hydrogen bond, it sterically occludes space, which becomes inaccessible to any other molecule [33]. The effective particle volume was calculated as

$$V^{ef} = \frac{1}{\rho} - \frac{\bar{n} V'}{2}, \tag{12}$$

where $V'$ is the volume not accessible to other molecules when two molecules form a hydrogen bond and can be approximated by simple geometry. Two water molecules that form a hydrogen bond are separated by a distance 1. If the LJ core is approximated by the diameter $d$ of HD molecules from BH perturbation theory, $V'$ can be approximated as

$$V' = \sqrt{d^2 - \frac{1}{2}} - \frac{\pi d^2}{4}. \tag{13}$$

In Eq. (12), $\bar{n}$ is the average number of hydrogen bonds per molecule. Each particle has four arms. The probability that a hydrogen bond is formed at one arm is $(1 - x)$, where $x$ is the ratio of nonbonded molecules at one arm. We now get

$$\bar{n} = 4(1 - x). \tag{14}$$

The effective particle density is calculated as

$$\rho^{ef} = \frac{1}{V^{ef}}. \tag{15}$$

The set of Eqs. (10)–(15) must be solved iteratively to get the effective density $\rho^{ef}$ and the fraction of molecules $x$ that are not hydrogen bonded. The effective packing fraction is then calculated as $\eta^{ef} = \rho^{ef} \pi d^2/4$. Once the effective density and packing fraction are known, the Helmholtz free energy can be calculated with Eqs. (7)–(9). In both versions of TPT, once the Helmholtz free energy is known, other thermodynamic quantities may be calculated using standard thermodynamic relations [49].

### C. Integral equation theory

In this section we briefly overview the orientationally averaged version of the multidensity Ornstein-Zernike (OZ) equation with the polymer Percus-Yevick (PPY) closure [31,41,52]. An extensive description of the theory was given in an MB paper [31]. The orientation averaging of the OZ equation is an additional approximation of the theory not present in the molecular dynamics studies. An advantage of this approximation is that it allows a relatively simple numerical evaluation of the structural and thermodynamic properties.

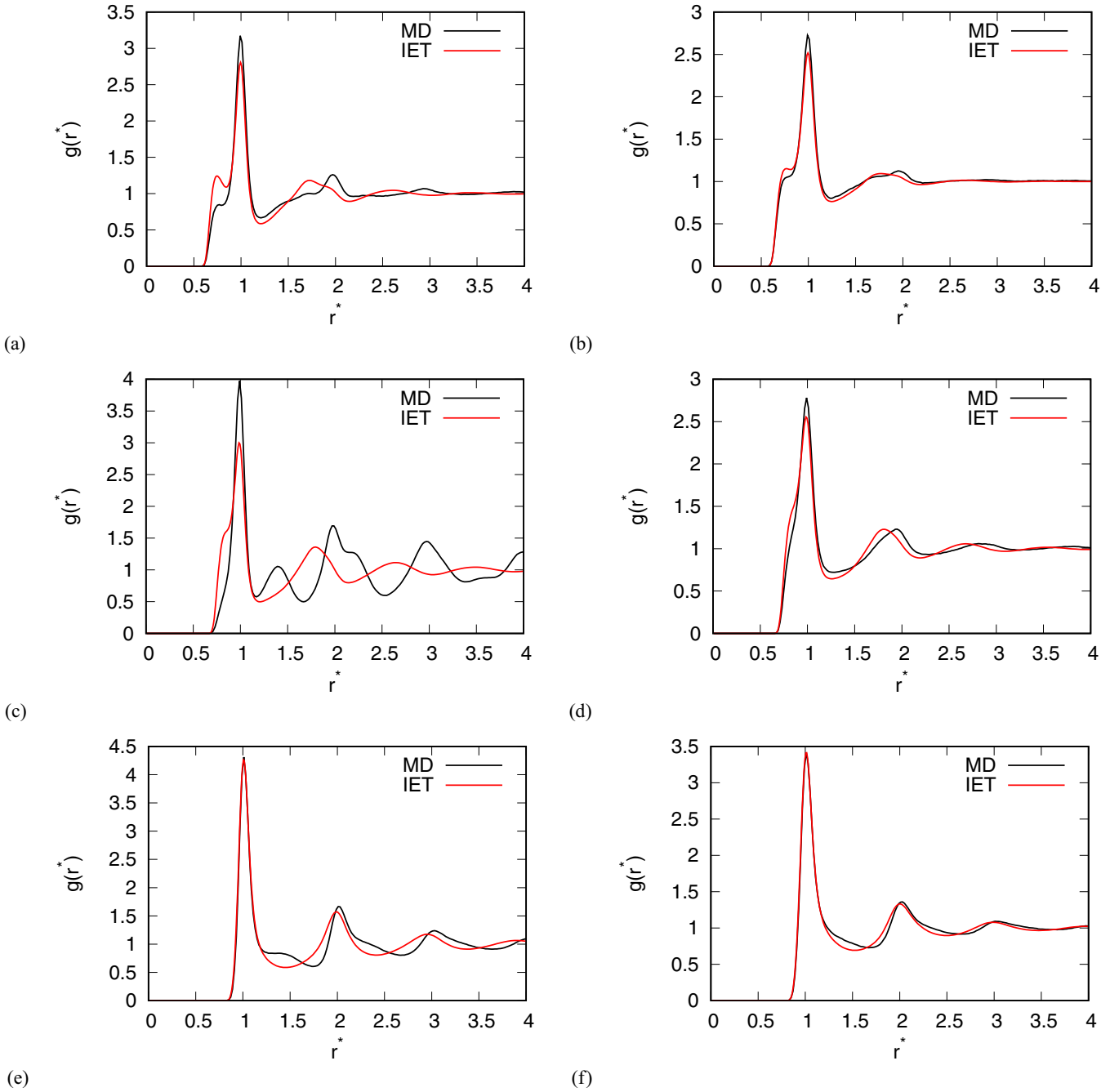


FIG. 8. Comparison of pair correlation functions for (a) $\sigma_{LJ} = 0.7$, $p^* = 0.19$, $T^* = 0.3$; (b) $\sigma_{LJ} = 0.7$, $p^* = 0.19$, $T^* = 0.4$; (c) $\sigma_{LJ} = 0.8$, $p^* = 0.5$, $T^* = 0.3$; (d) $\sigma_{LJ} = 0.8$, $p^* = 0.5$, $T^* = 0.4$; (e) $\sigma_{LJ} = 1.0$, $p^* = 0.75$, $T^* = 0.35$; and (f) $\sigma_{LJ} = 1.0$, $p^* = 0.75$, $T^* = 0.45$.

The multidensity OZ equation for the model described is written as

$$\hat{\mathbf{h}}(k) = \hat{\mathbf{c}}(k) + \hat{\mathbf{c}}(k)\boldsymbol{\rho}\hat{\mathbf{h}}(k) \tag{16}$$

where $\hat{\mathbf{h}}(k)$ and $\hat{\mathbf{c}}(k)$ are the matrices whose elements are the Fourier transforms of the partial correlation functions $h_{ij}(r)$ and $c_{ij}(r)$. We use partial correlation functions which remain finite upon decrease of the temperature [31]. In Eq. (16) $\boldsymbol{\rho}$ represents the matrix which replaces the Wertheim density parameters $\sigma$ and contains the partial number densities. In the calculations we restrict ourselves to the so-called "ideal network" approximation [52,53]. This means that we neglect the part of the correlation responsible for formation of the ring-like structures [52]. Originally the OZ equation involves the matrices $\mathbf{c}$, $\mathbf{h}$, and $\boldsymbol{\rho}$ of dimensionality $5 \times 5$. By taking into account the equivalence of the bonding arms we obtain

$$\hat{\mathbf{w}}(k) = \begin{pmatrix} \hat{w}_{00}(k) & \hat{w}_{01}(k) \\ \hat{w}_{10}(k) & \hat{w}_{11}(k) \end{pmatrix}, \tag{17}$$

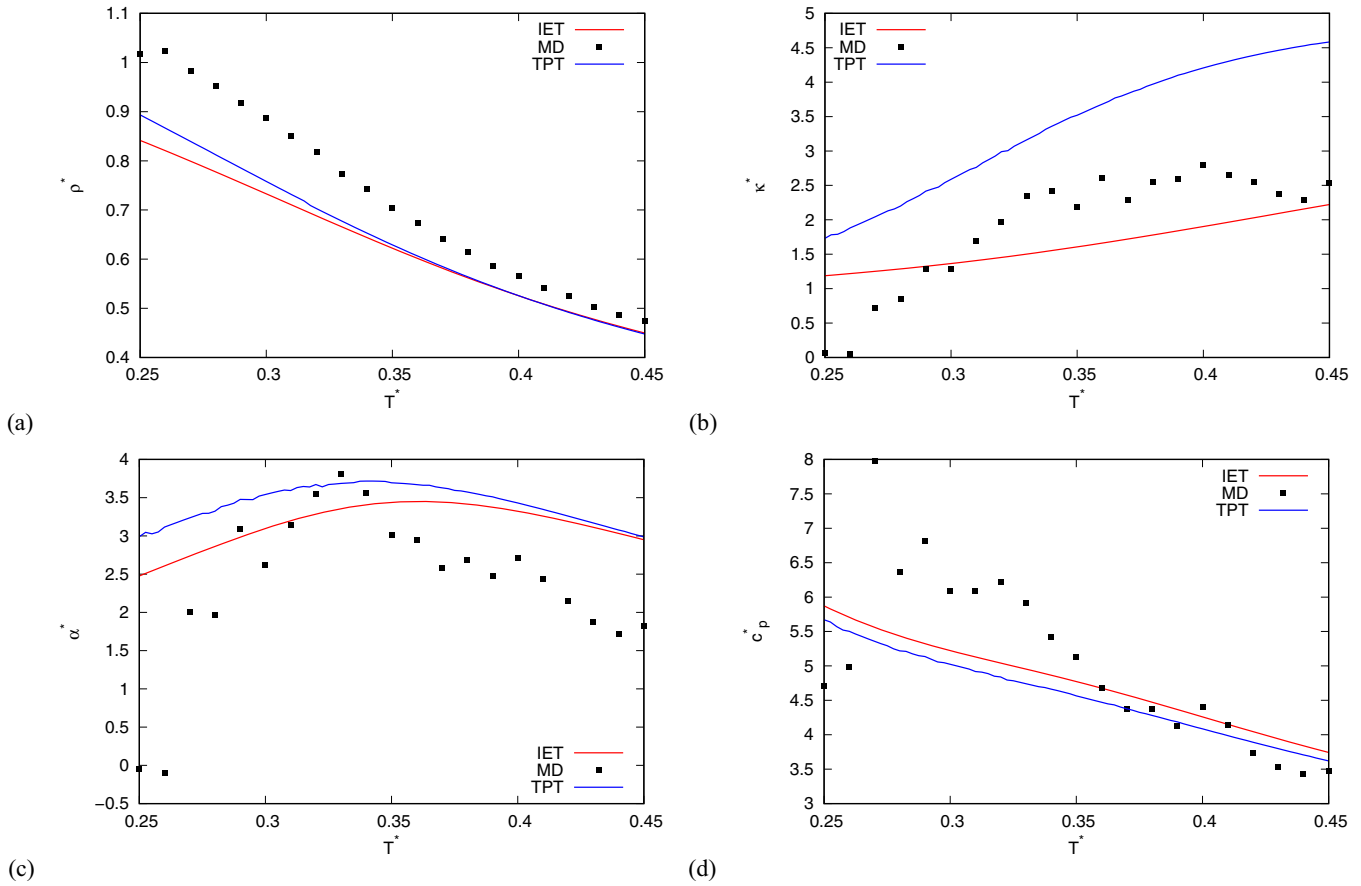


FIG. 9. Comparison of temperature dependence of (a) the density, (b) the isothermal compressibility multiplied by pressure, (c) the thermal expansion coefficient, and (d) the heat capacity for various pressures for $\sigma_{\mathrm{LJ}} = 0.7$ and $p^* = 0.19$ between molecular dynamics results and results of both theories.

where $w$ stands for either the $h$ or $c$ correlation function, and $\boldsymbol{\rho}$ is the matrix containing the partial densities,

$$\rho = \begin{pmatrix} \rho & 4\rho \\ 4\rho & 12\rho \end{pmatrix}. \tag{18}$$

The coefficients 4 and 12 in $\boldsymbol{\rho}$ result from the reduction of the dimensionality of the OZ equation [31]. In order to solve the OZ equation an additional relation between the $h$ and $c$ correlation functions is needed. In the present study we choose the PPY closure [41] in the form

$$\begin{aligned} c_{ij}(r) = {} & f_{\mathrm{LJ}}(r)[t_{ij}(r) + \delta_{i0}\delta_{j0}] \\ & + \delta_{i1}\delta_{j1}x^2 \bar{f}_{\mathrm{HB}}(r) e_{\mathrm{LJ}}(r)[t_{00}(r) + 1], \end{aligned} \tag{19}$$

where $t(r) = h(r) - c(r)$, $x$ is the fraction of particles not bonded at one arm, $f_{\mathrm{LJ}}(r) = e_{\mathrm{LJ}}(r) - 1$, and $e_{\mathrm{LJ}}(r) = \exp[-\beta U_{\mathrm{LJ}}(r)]$. Furthermore, $\bar{f}_{\mathrm{HB}}(r)$ is the orientationally averaged Mayer function for the hydrogen-bond potential between arms of two different particles [Eq. (3)] and $x$ follows from mass-action law as given by Eq. (10). The total pair distribution function $g(r)$ is calculated via the relations

$$g(r) = g_{00}(r) + 4g_{01}(r) + 4g_{10}(r) + 16g_{11}(r). \tag{20}$$

The OZ equation together with the PPY closure condition is solved by a direct iteration. The forward and inverse Bessel-Fourier transforms, needed to couple the correlation functions in real and Fourier spaces, have been performed by the method of Talman [54]. Once the pair correlation function is known other thermodynamic properties can be calculated with standard thermodynamic relations [31].

## IV. RESULTS AND DISCUSSION

All the results are presented in dimensionless units, normalized to the strength of the optimal HB $\epsilon_{\mathrm{HB}}$ and HB separation $r_{\mathrm{HB}}$. ($T^* = k_B T/|\epsilon_{\mathrm{HB}}|$, $u^{ex*} = u^{ex}/|\epsilon_{\mathrm{HB}}|$, $V^* = V/r_{\mathrm{HB}}^2$, and $p^* = pr_{\mathrm{HB}}^2/|\epsilon_{\mathrm{HB}}|$).

As first we checked properties of the model and presence of density maxima for different types of the potential, the distance of the hydrogen bond in comparison to the Lennard-Jones core. To do this we have varied parameter $\sigma_{\mathrm{LJ}}$. Thermodynamics properties including density $\rho^*$, thermal expansion coefficient $\alpha^*$, isothermal compressibility $\kappa^*$, and heat capacity at constant pressure $c_p^*$ are plotted in Figs. 2–5 for different sizes of the Lennard-Jones core. The interplay of long-range opened structures and short-range closed packed structures results in density maxima. The density maxima can be observed for cores smaller than 1.0 ($\sigma_{\mathrm{LJ}} < 1.0$). For size $\sigma_{\mathrm{LJ}} = 0.9$ the density maxima is still present (see Fig. 4) while for size $\sigma_{\mathrm{LJ}} = 1.0$ it is already gone (see Fig. 5). An increase in size of the LJ core moves the density maxima to higher temperatures and pressures as well as shifts the melting point

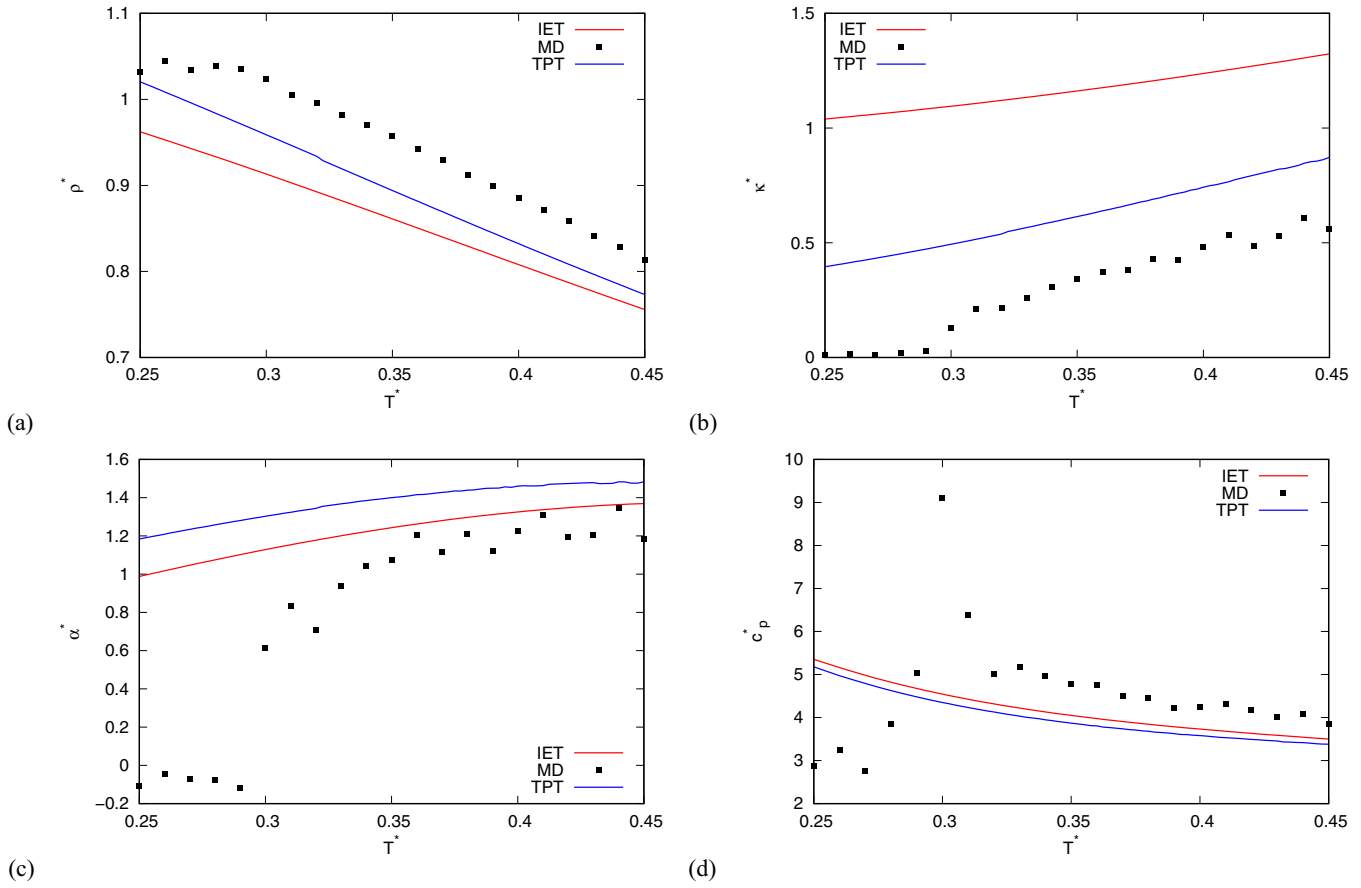


FIG. 10. Comparison of temperature dependence of (a) the density, (b) the isothermal compressibility multiplied by pressure, (c) the thermal expansion coefficient, and (d) the heat capacity for various pressures for $\sigma_{\mathrm{LJ}} = 0.8$ and $p^* = 0.5$ between molecular dynamics results and results of both theories.

to higher temperatures. For the thermal expansion coefficient we observe negative values on the left of the density maxima. Heat capacity at constant pressure is high but it decreases with increasing pressure. The decrease of heat capacity with increasing pressure is due to smaller possible states available in highly dense liquid. There is a high peak present close to the melting point. The isothermal compressibility is rather low at high pressure and high for low pressure. In solid state it is almost zero. The density maxima is most pronounced at a size of LJ core around 0.8. Figure 6 shows some snapshots of the typical structures for a small size of LJ core where density maxima is most pronounced. Figure 6(a) shows the typical structures at low temperature and Fig. 6(b) at high temperature. At low temperature the system is in liquid phase while at high temperature we have a gas phase. In Fig. 6(c) we have a snapshot of the system with LJ core $\sigma_{\mathrm{LJ}} = 0.8$ at temperature and pressure of density maxima. We can observe a lot of square cell structures as well as close contacts. At lower temperatures than this point there are more square cell structures present, leading to lower density, while at higher temperatures these HB structures are melting, which again leads to lower density. In Fig. 6(d) we can see these structures. In all the figures we can see that BN4 particles form a lot of hydrogen bonds and ring structures.

In comparison to the 2D MB model we have observed the following differences for size of core 0.7. The melting point for BN4 is higher than for the MB model (see Fig. 7); for the MB model it is around $T^* = 0.15$, while for BN4 it is around $T^* = 0.25$. The density for the BN4 model is higher than for the MB model at the same temperature and pressure. BN4 does not have density maxima at this pressure. At all temperatures the density of the BN4 model is higher because the crystal phase of the MB model has more empty spaces. The crystal phase of BN4 has cubic symmetry while the MB model has hexagonal symmetry. The BN4 model freezes in crystal structure with less defects than the MB model.

In continuation of our study we first check how well the structure of the BN4 model can be reproduced by IET by calculating pair correlation functions. Figure 8 shows a comparison of correlation functions for different sizes and state points obtained by molecular dynamics and IET. At high temperatures the IET is able to reproduce the structure rather well, while at lower temperature only for bigger cores. For a size of core equal to $\sigma_{\mathrm{LJ}} = 0.8$ the IET is failing to predict correct positions and highs of peaks at low temperatures. There are two reasons for this. One is that we are neglecting formation of ring structures in IET. The second

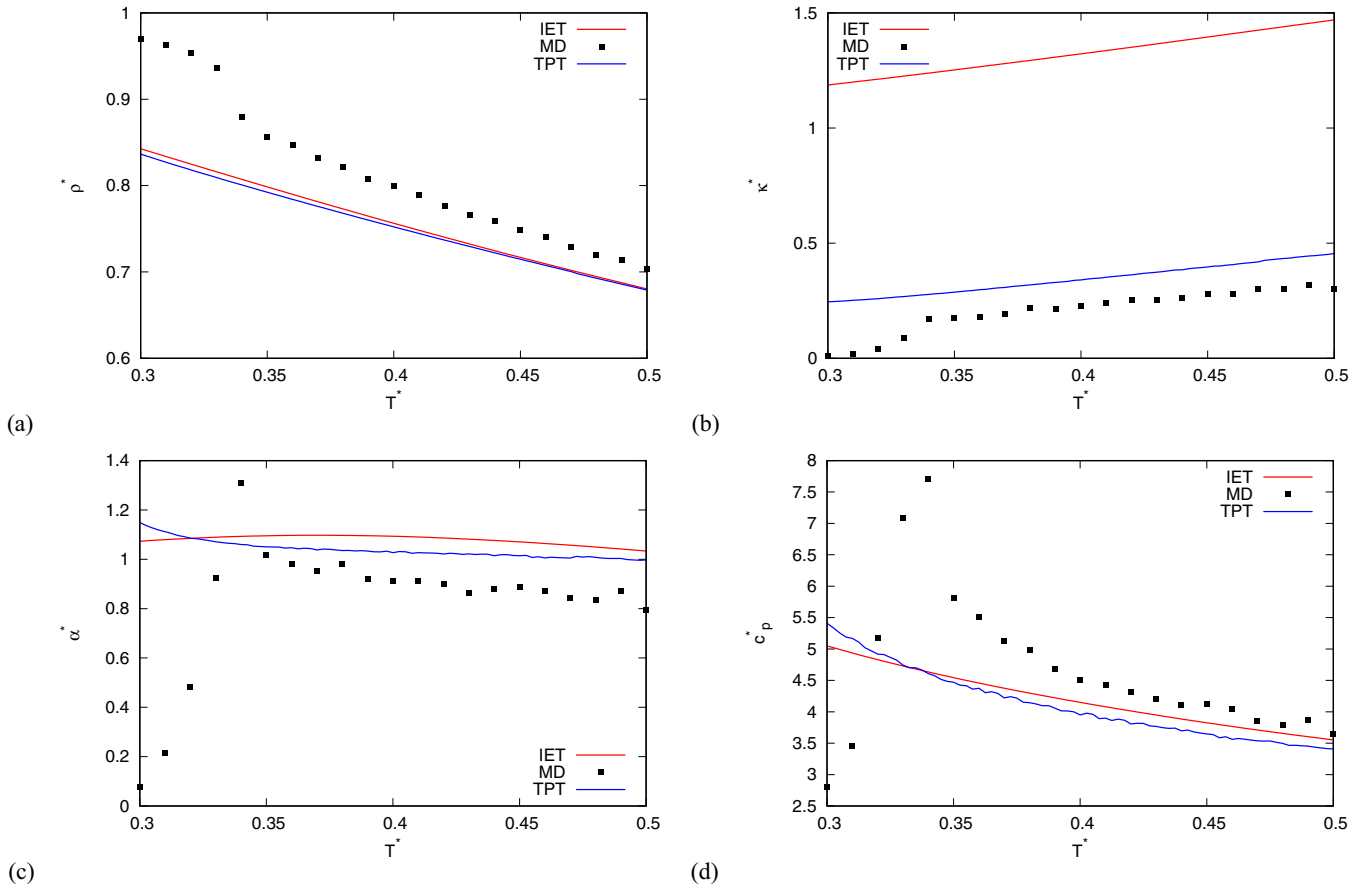


FIG. 11. Comparison of temperature dependence of (a) the density, (b) the isothermal compressibility multiplied by pressure, (c) the thermal expansion coefficient, and (d) the heat capacity for various pressures for $\sigma_{\mathrm{LJ}} = 1.0$ and $p^* = 0.75$ between molecular dynamics results and results of both theories.

reason is orientational averaging. We are treating HBs in an averaged way. This approximation is equivalent to forming HB at a random angle. This approximation is okay at high temperatures and high sizes. At low temperatures and small sizes this is no longer valid. It is also interesting to see that at even smaller sizes ($\sigma_{\mathrm{LJ}} = 0.7$) the agreement improves.

At the end, we have also verified how well both theories, IET and TPT, can properly predict thermodynamics properties (see Figs. 9–11). Both theories correctly predict trends. Like in the case of pair correlation function, the biggest error is at size $\sigma_{\mathrm{LJ}} = 0.8$. Both theories failed to predict density maxima for all sizes like it was observed for the MB model [31]. For density dependence both theories have the proper trend but it looks like they have a systematic error. This is different than observed for the MB model [31], where the IET and TPT results are not shifted in comparison to computer simulations. The best agreement is for heat capacity and thermal expansion at higher temperatures. At low temperatures both fail in predicting negative thermal expansion. The BN4 model has very low compressibility due to close packed square structures and the theories are not able to account for this.

## V. CONCLUSIONS

We have determined properties of the BN4 model by molecular dynamics and two statistical-mechanical theories developed for associated fluids by Wertheim. The BN4 model balances Lennard-Jones interactions with an orientation dependence that is intended to mimic hydrogen bonding. The BN4 model has volume anomalies like real water. The IET is somewhat more demanding from a computational point of view than the TPT, but both are orders of magnitude more efficient than the computer simulations. Both theories qualitatively reproduce the temperature trends of key thermodynamic properties like molar volume, isothermal compressibility, thermal expansion coefficient, and heat capacity. Both theories improve at high temperatures, where the orientational averaging approximation is least problematic.

## ACKNOWLEDGMENTS

The financial support of the Slovenian Research Agency through Grant No. P1-0201 as well as Projects No. N1-0186, No. L2-3161, and No. and J4-4562 is acknowledged, as well as National Institutes for Health RM1 Award No. RM1GM135136.

[1] M. Chaplin, Nat. Rev. Mol. Cell Biol. **7**, 861 (2006).
[2] M. J. Tait and F. Franks, Nature (London) **230**, 91 (1971).
[3] P. Gallo, K. Amann-Winkel, C. A. Angell, M. A. Anisimov, F. Caupin, C. Chakravarty, E. Lascaris, T. Loerting, A. Z. Panagiotopoulos, J. Russo, J. A. Sellberg, H. E. Stanley, H. Tanaka, C. Vega, L. Xu, and L. G. M. Pettersson, Chem. Rev. **116**, 7463 (2016).
[4] E. Brini, C. J. Fennell, M. Fernandez-Serra, B. Hribar-Lee, M. Luksic, and K. A. Dill, Chem. Rev. **117**, 12385 (2017).
[5] *Water a Comprehensive Treatise Vol. 7* (Water and Aqueous Solutions at Subzero Temperatures), edited by F. Franks (Plenum Press, New York, 1982).
[6] D. Eisenberg and W. Kauzmann, *The Structure and Properties of Water* (Oxford University Press, Oxford, 1969).
[7] J. M. Kincaid and G. Stell, Phys. Lett. A **65**, 131 (1978).
[8] P. Lamparter, S. Stieb, and W. Knoll, Z. Naturforsch. A **31**, 90 (1976).
[9] H. Thurn and J. Ruska, J. Non-Cryst. Solids **22**, 331 (1976).
[10] G. E. Sauer and L. B. Borst, Science **158**, 1567 (1967).
[11] W. L. Jorgensen, J. Chandrasekhar, J. D. Madura, R. W. Impey, and M. L. Klein, J. Chem. Phys. **79**, 926 (1983).
[12] I. Nezbeda, J. Mol. Liq. **73–74**, 317 (1997).
[13] B. Guillot, J. Mol. Liq. **101**, 219 (2002).
[14] C. Vega, J. L. F. Abascal, M. M. Conde, and J. L. Aragones, Faraday Discuss. **141**, 251 (2009).
[15] F. H. Stillinger, Science **209**, 451 (1980).
[16] C. Tanford, *The Hydrophobic Effect: Formation of Micelles and Biological Membranes*, 2nd ed. (Wiley, New York, 1980).
[17] W. Blokzijl and J. B. F. N. Engberts, Angew. Chem. Int. Ed. Engl. **32**, 1545 (1993).
[18] G. Robinson, S.-B. Zhu, S. Singh, and M. Evans, *Water in Biology, Chemistry and Physics: Experimental Overviews and Computational Methodologies* (World Scientific, Singapore, 1996).
[19] R. Schmid, Monatshefte für Chemie **132**, 1295 (1993).
[20] A. Ben-Naim, Biophys. Chem. **105**, 183 (2003).
[21] L. R. Pratt, Annu. Rev. Phys. Chem. **53**, 409 (2002).
[22] K. B. Lipkowitz, D. B. Boyd, S. J. Smith, and B. T. Sutcliffe, Rev. Comput. Chem. **10**, 271 (2007).
[23] E. J. Baerends and O. V. Gritsenko, J. Phys. Chem. A **101**, 5383 (1997).
[24] T. M. Truskett, P. G. Debenedetti, S. Sastry, and S. Torquato, J. Chem. Phys. **111**, 2647 (1999).
[25] K. A. Dill, T. M. Truskett, V. Vlachy, and B. Hribar-Lee, Annu. Rev. Biophys. Biomol. Struct. **34**, 173 (2005).
[26] I. Nezbeda, J. Kolafa, and Yu. V. Kalyuzhnyi, Mol. Phys. **68**, 143 (1989).
[27] I. Nezbeda and G. A. Iglezias-Silva, Mol. Phys. **69**, 767 (1990).
[28] K. A. T. Silverstein, A. D. J. Haymet, and K. A. Dill, J. Am. Chem. Soc. **120**, 3166 (1998).
[29] A. Ben-Naim, J. Chem. Phys. **54**, 3682 (1971).
[30] A. Ben-Naim, Mol. Phys. **24**, 705 (1972).
[31] T. Urbič, V. Vlachy, Yu. V. Kalyuzhnyi, N. T. Southall, and K. A. Dill, J. Chem. Phys. **112**, 2843 (2000).
[32] T. Urbič, V. Vlachy, Yu. V. Kalyuzhnyi, N. T. Southall, and K. A. Dill, J. Chem. Phys. **116**, 723 (2002).
[33] T. Urbič, V. Vlachy, Yu. V. Kalyuzhnyi, and K. A. Dill, J. Chem. Phys. **127**, 174511 (2007).
[34] T. Urbič, V. Vlachy, Yu. V. Kalyuzhnyi, and K. A. Dill, J. Chem. Phys. **118**, 5516 (2003).
[35] T. Urbič, V. Vlachy, O. Pizio, and K. A. Dill, J. Mol. Liq. **112**, 71 (2004).
[36] T. Urbič and M. F. Holovko, J. Chem. Phys. **135**, 134706 (2011).
[37] T. Urbič and K. A. Dill, J. Chem. Phys. **132**, 224507 (2010).
[38] T. Urbič, Phys. Rev. E **85**, 061503 (2012).
[39] T. Urbič, Phys. Rev. E **94**, 042126 (2016).
[40] T. Urbič, Phys. Rev. E **96**, 032122 (2017).
[41] M. S. Wertheim, J. Stat. Phys. **42**, 459 (1986).
[42] M. S. Wertheim, J. Chem. Phys. **87**, 7323 (1987).
[43] E. A. Muller and K. E. Gubbins, in *IUPAC Volume on Equations of State for Fluids and Fluid Mixtures*, edited by J. V. Sengers, M. B. Ewing, R. F. Kayser, and C. J. Peters (Blackwell Scientific, Hoboken, 1999).
[44] Yu. V. Kalyuzhnyi, and P. T. Cummings, in *IUPAC Volume on Equations of State for Fluids and Fluid Mixtures*, edited by J. V. Sengers, M. B. Ewing, R. F. Kayser, and C. J. Peters (Blackwell Scientific, Hoboken, 1999).
[45] M. S. Wertheim, J. Chem. Phys. **88**, 1145 (1987).
[46] M. S. Wertheim, J. Chem. Phys. **85**, 2929 (1986).
[47] W. C. Swope, H. C. Andersen, P. H. Berens, and K. R. Wilson, J. Chem. Phys. **76**, 637 (1982).
[48] H. J. C. Berendsen, J. P. M. Postma, W. F. van Gunsteren, A. DiNola, and J. R. Haak, Molecular dynamics with coupling to an external bath, J. Chem. Phys. **81**, 3684 (1984).
[49] J. P. Hansen and I. R. McDonald, *Theory of Simple Liquids* (Academic, London, 1986).
[50] D. Frenkel and B. Smit, *Molecular Simulation: From Algorithms to Applications*, (Academic Press, New York, 2000).
[51] G. Jackson, W. G. Chapman, and K. E. Gubbins, Mol. Phys. **65**, 1 (1988).
[52] E. V. Vakarin, Yu. Ja. Duda, and M. F. Holovko, Mol. Phys. **90**, 611 (1997).
[53] J. Chang and S. I. Sandler, J. Chem. Phys. **102**, 437 (1995).
[54] J. D. Talman, J. Comput. Phys. **29**, 35 (1978).